

# Results of DVCS Measurement at COMPASS

Johannes GIARRA<sup>1</sup> on behalf of the COMPASS Collaboration

<sup>1</sup>*Institute for nuclear physics, Johannes Gutenberg-University, 55128 Mainz, Germany*

*E-mail: jgiarra@cern.ch*

(Received February 5, 2022)

Deeply Virtual Compton Scattering (DVCS) is the golden exclusive reaction to study Generalized Parton Distributions (GPDs). Such exclusive measurements were performed at COMPASS in 2016 and 2017 at the M2 beamline of the CERN SPS using the 160 GeV muon beam scattering off a 2.5 m long liquid hydrogen target surrounded by a barrel-shaped time-of-flight system to detect the recoiling target proton. The scattered muons and the produced real photons were detected by the COMPASS spectrometer, which was supplemented by an additional electromagnetic calorimeter for the detection of large-angle photons. The DVCS cross section and its dependence with respect to the squared four-momentum transfer are extracted from the sum of cross-sections measured with opposite beam charge and polarization. The goal of the measurement is to determine the transverse extension of the partons in the specific Bjorken  $x$  domain of COMPASS between valence quarks and gluons. The analysis method and preliminary results of the long run will be discussed.

**KEYWORDS:** Muon scattering, DVCS, GPDs

## 1. Introduction

General Parton Distribution functions (GPDs) describe the three-dimensional structure of the nucleon, correlating the transverse spatial distributions of the partons with their longitudinal momenta inside the nucleon. A way of constraining these functions is to study hard exclusive photon production including Deeply Virtual Compton Scattering (DVCS) or Hard Exclusive Meson Production (HEMP). A test measurement of DVCS in 2012, followed up by dedicated measurements in 2016/17, was performed at COMPASS. The following sections give a brief overview of the ongoing analysis of the 2016/17 data including preliminary results on the DVCS cross section.

## 2. The COMPASS Experiment

COMPASS (COMmon Muon Proton Apparatus for Structure and Spectroscopy) is a fixed-target experiment located at the M2 beamline of the Super Proton Synchrotron (SPS) at CERN [1, 2]. The beamline is able to deliver different types of high energy hadron and lepton beams, enabling COMPASS to perform scattering and spectroscopic measurements on a variety of targets. The spectrometer consists of two stages, which are build around the two spectrometer magnets. In the first stage behind the target particles at large scattering angle are measured, while the second stage, following further downstream with respect to the target, measures particles at small scattering angles.

For the measurement performed in 2016/17 a 160 GeV muon beam was scattered off a 2.5 m long liquid hydrogen ( $\text{IH}^2$ ) target. The muon beam is produced via the weak decay of charged pions and kaons, which emerge from a collision of a proton beam on a beryllium target. Due to the weak decay the positively and negatively charged muons have opposite polarization. To perform an exclusive measurement of the DVCS process ( $\mu + p \rightarrow \mu' + p' + \gamma$ ), the COMPASS spectrometer was supplemented by an electromagnetic calorimeter and a recoil proton detector. Its two concentric cylinders,

made of scintillator slats, surround the  $\text{IH}^2$  target performing a Time-of-Flight (ToF) measurement of the scattered proton between the inner and the outer ring. The acceptance for real photons with large scattering angles was increased by placing in addition to the already present calorimeters (ECAL1 and ECAL2) in each stage, another calorimeter (ECAL0) directly behind the target. The events are recorded by using a trigger system, which is dedicated to trigger on the scattered muons. The identification of the scattered muons is performed by using a setup of small area and large area tracking detectors interleaved with absorbers.

### 3. Measurement of Deeply Virtual Compton scattering at COMPASS

The DVCS study at COMPASS [3] is focused on extracting the GPD  $H$  via the related and experimentally accessible Compton Form Factor (CFF)  $\mathcal{H}$ . A way of accessing the DVCS contribution in the measured cross section of the exclusive photon production is by exploiting the opposite polarization of the positively and negatively charged muon beams. This allows to determine the charge-spin cross-section sum [4]:

$$\mathcal{S}_{CS,U} \equiv d\sigma^{\leftarrow\pm} + d\sigma^{\rightarrow\pm} = 2(d\sigma^{BH} + d\sigma^{DVCS} - |P_\mu|d\sigma^I). \quad (1)$$

Here  $\pm$  refers to the charge, while  $\leftarrow$ ,  $\rightarrow$  and  $|P_\mu|$  to the polarization of the muon beam.  $d\sigma$  abbreviates as:

$$d\sigma^\pm = \frac{d^4(\sigma^{\mu+p \rightarrow \mu'+p'+\gamma})^\pm}{dQ^2 dv dt |d\phi},$$

where  $Q^2$  is the virtuality of the exchanged photon,  $\nu$  is its energy,  $t$  is the squared four-momentum transfer to the recoil proton and  $\phi$  is the azimuthal angle between the lepton scattering and photon production plane.

The three terms in equation 1 refer to the contributions by the DVCS process, the Bethe-Heitler ( $BH$ ) process and the interference ( $I$ ) of both processes. At sufficiently large  $Q^2$  and small  $|t|$ , the azimuthal dependence of the DVCS cross section and the interference term including twist-3 contributions reads as [4, 5]:

$$d\sigma^{DVCS} \propto \frac{1}{y^2 Q^2} (c_0^{DVCS} + c_1^{DVCS} \cos \phi + c_2^{DVCS} \cos 2\phi) \text{ and}$$

$$d\sigma^I \propto \frac{1}{x_B y^3 t P_1(\phi) P_2(\phi)} (s_1^I \sin \phi + s_2^I \sin 2\phi),$$

where  $P_1(\phi)$  and  $P_2(\phi)$  are the  $BH$  lepton propagators,  $y$  the virtual photon energy with respect to the beam energy, and  $c_i^{DVCS}$  and  $s_i^I$  are combinations of CFFs [5]. The contribution of the interference term is suppressed by integrating the differential cross sections over  $\phi$ . By this the contribution of the term  $c_0^{DVCS}$  is selected, which is dominated by the imaginary part of CFF  $\mathcal{H}$  and can be related to the transverse extension of partons in the proton via the exponential  $|t|$ -dependence of the cross section.

### 4. Extraction of the $|t|$ -dependent DVCS cross section

The DVCS cross section is extracted in bins of  $|t|$ ,  $\nu$ ,  $Q^2$  and  $\phi$  separately for each beam charge. The cross section in each bin is given as:

$$\left\langle \frac{d\sigma_{DVCS}}{d|t|d\phi dQ^2 dv} \right\rangle_{t_i\phi_j Q_k^2 \nu_l}^\pm = \frac{1}{\mathcal{L}^\pm \Delta t_i \Delta \phi_j \Delta Q_k^2 \Delta \nu_l} \left[ (a_{ijkl}^\pm)^{-1} (data - BH_{MC} - \pi_{MC}^0) \right] \quad (2)$$

Here  $\mathcal{L}^\pm$  denotes the integrated luminosity and  $a^\pm$  the acceptance. The first term in the last bracket refers to the amount of observed single photon events, which are determined by an dedicated event selection. As mentioned before this cross section also includes a contribution by the Bethe-Heitler process ( $BH_{MC}$ ) and in addition also a background from the decay of  $\pi^0 \rightarrow \gamma\gamma$  contaminating the exclusive photon data sample ( $\pi_{MC}^0$ ). Their corresponding contributions, noted  $MC$ , are determined by using dedicated Monte-Carlo samples.

The selection of the exclusive photon events follows strict selection criteria to identify the vertex candidates and the corresponding real photon and recoil proton candidates. The vertex candidates in the target material are selected by identifying an incoming and scattered muon. For the real photon selection the energy of the corresponding calorimeter cluster has to be above a certain high energy threshold, which are chosen for each ECAL according to the simulated DVCS photon distribution. The recoil proton candidates are measured and identified by the recoil detector. The event selection is further improved by removing non-exclusive events based on exclusivity conditions and performing a kinematic fit under the assumption of exclusive photon production. As the measurement of the exclusive photon events is over-constrained, so-called exclusivity conditions are formulated, which compare the measurement of the spectrometer and recoil detector. Using a kinematic fit improves the resolution of kinematic variables especially in  $|t|$  and  $\nu$ . In the end only those events are included in the analysis, which have only a single combination of vertex candidate, real photon and proton candidate left that fulfills all selection criteria.

Great effort has been put not only on checking and improving the quality of real data but also on improving its agreement with simulated data. This good agreement is mandatory for achieving a precise estimation of the BH contribution and  $\pi^0$  contamination. The exclusive photon events are generated by the HEPGEN event generator, which includes a description of the BH process based on QED predictions and the known proton form factors. Using the measured luminosity the BH events can be subtracted from the data. As mentioned above the main background contamination is due to  $\pi^0$  decays. One part of this contamination can be directly identified and then removed from data (visible  $\pi^0$ ). This comprises all  $\pi^0$  decays where both decay photons are detected. By combining the high energy photon with all low energy photons within the same event, those photon pairs with an invariant mass ( $M_{\gamma\gamma}$ ) in the  $\pm 20$  MeV range around the nominal  $\pi^0$  mass are considered to be a  $\pi^0$ . In other cases the second photon escaped the detection, which makes it impossible to identify the corresponding  $\pi^0$  event in the data (invisible  $\pi^0$ ). To estimate this contamination two Monte-Carlo samples, one dedicated to the exclusive and another one to inclusive  $\pi^0$  production, are used. The exclusive production channel is covered by the HEPGEN generator, which includes a model from Goloskokov and Kroll (GK) [6]. In case of the inclusive produced  $\pi^0$ , the LEPTO 6.1 generator is used, which simulates the hadronization based on the Lund string model [7]. To estimate the invisible  $\pi^0$  contamination, the same selection as for the exclusive photon events is performed. The normalization to the real data is done by normalizing the visible  $\pi^0$  in the Monte-Carlo samples to the visible  $\pi^0$ , which are present in the real data. The relative fraction of the two Monte-Carlo samples is estimated by fitting kinematic distributions of the real data, obtained by a dedicated  $\pi^0$  selection, to the corresponding distributions in both  $\pi^0$  Monte-Carlo samples.

Fig. 1 shows the  $\phi$ -distributions of exclusive single photon events in three  $\nu$ -domains using approximately 30% of the available data in 2016/17. In the region of high  $\nu$  and relative small  $x_{Bj}$  (left plot) the BH process is the dominant one. A good agreement ( $98.6 \pm 1\%$ ) between the data and the BH Monte-Carlo is obtained. The good description of the BH at large  $\nu$  allows to subtract its contribution in the other  $\nu$  regions. At low  $\nu$  ( $10 \text{ GeV} < \nu < 32 \text{ GeV}$ ) a sizable DVCS contribution is observed, which is used to extract the  $|t|$ -dependence of the DVCS cross section.

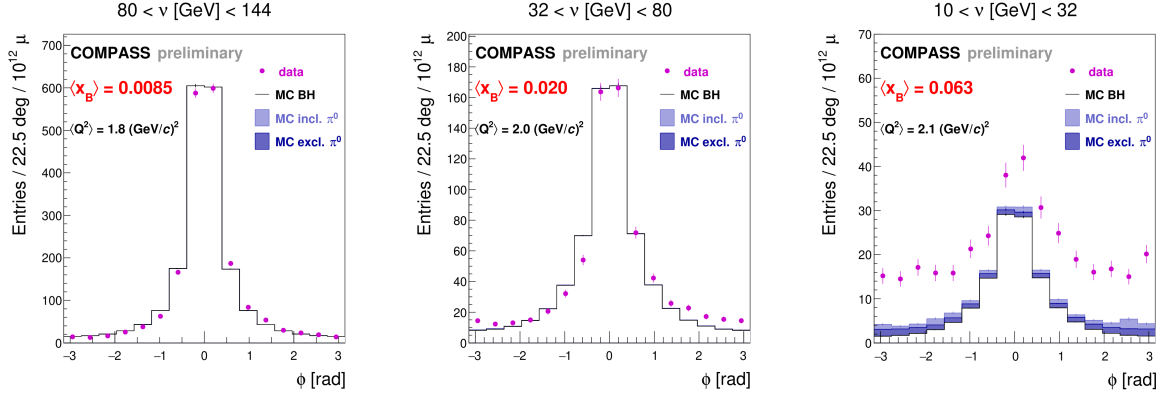


**Fig. 1.** The  $\phi$ -distribution of the exclusive photon events in three different  $\nu$ -domains. The data for both beam polarization is shown as solid points, the contribution of the BH Monte-Carlo is indicated by the black line and the estimated inclusive and exclusive invisible  $\pi^0$  contaminations are given by the light and dark shaded areas. The visible  $\pi^0$  contamination is already removed.

## 5. Extraction of the slope parameter $B$

The sum of the charge separated cross section:

$$\left\langle \frac{d\sigma_{DVCS}}{d|t|} \right\rangle_{t_i} = \frac{1}{2} \left( \left\langle \frac{d\sigma_{DVCS}}{d|t|} \right\rangle_{t_i}^+ + \left\langle \frac{d\sigma_{DVCS}}{d|t|} \right\rangle_{t_i}^- \right), \quad (3)$$

is calculated in the kinematic domain of  $1 \text{ (GeV/c)}^2 < Q^2 < 5 \text{ (GeV/c)}^2$ ,  $10 \text{ GeV} < \nu < 32 \text{ GeV}$  and 4 bins in  $|t|$ :

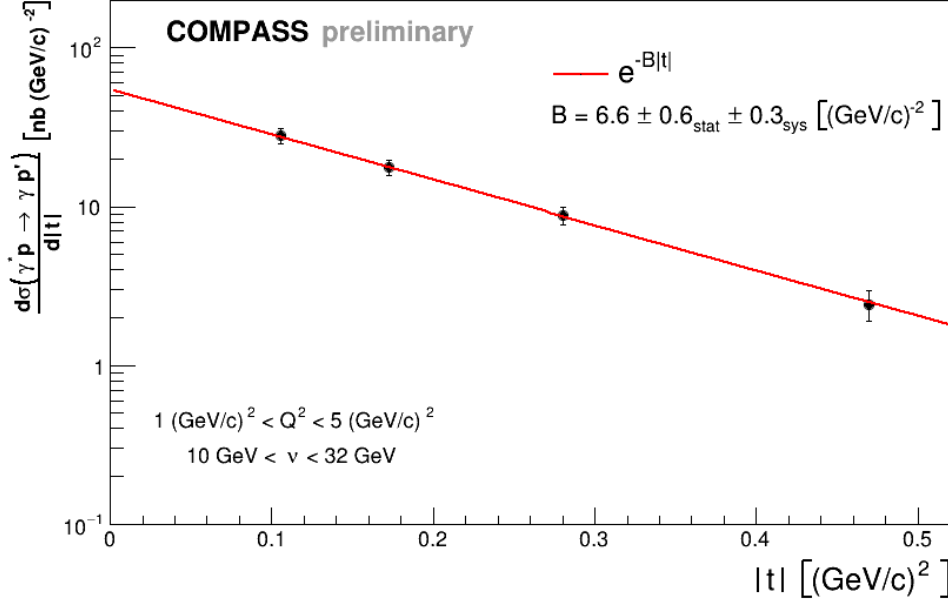
$$t_{i \in [1,4]}: [0.08-0.136], [0.136-0.219], [0.219-0.36], [0.36-0.64] \text{ (GeV/c)}^2.$$

Fig. 2 shows the preliminary result of the cross section and the statistical errors in each  $|t|$  bin, which clearly shows an exponential  $|t|$ -dependence.

The  $|t|$ -slope is fitted by a binned maximum Likelihood-fit using an exponential Ansatz of the form:  $e^{-B|t|}$ . The preliminary result on the  $B$ -parameter is:

$$B = (6.6 \pm 0.6_{stat} \pm 0.3_{sys}) \text{ (GeV/c)}^2.$$

The dominant source of systematic uncertainties to the  $B$  parameter is due to the normalization of the Monte-Carlo simulation to the visible  $\pi^0$  in real data.



**Fig. 2.** Cross section of the virtual-photon proton scattering in 4 bins of  $|t|$  with the corresponding statistical errors (black points). The  $|t|$ -dependence is described by a binned maximum Likelihood-fit using an exponential Ansatz of the form:  $e^{-B|t|}$  (red).

The data is marginally comparable with the published results obtained using the 2012 data [4], but a difference of approximately  $2.5\sigma$  is observed. In contrast to 2012 the intensities for both beam polarization are much more similar and a better agreement between both data sets is reached. The quality of the Monte-Carlo simulation was improved e.g. by including a more detailed description of the trigger and general detector performance. The event selection of 2012 was revised and some additional constraints were added.

To conclude on the result, more careful systematic checks are pending. For the moment only 2016 data was analyzed, but preparations of 2017 data are on going.

## References

- [1] COMPASS Collaboration, Nucl. Inst. Meth. Phys. Res. A: Accel. Spectrom. Detect. Assoc. Equip. **577**, pp. 455-518 (2007).
- [2] COMPASS Collaboration, Nucl. Inst. Meth. Phys. Res. A: Accel. Spectrom. Detect. Assoc. Equip. **779**, pp. 69-115 (2015).
- [3] COMPASS Collaboration, SPSC-P-340 (2010).
- [4] COMPASS Collaboration, Phys. Lett. B **793**, pp. 188-194 (2019).
- [5] A. V. Belitsky et al., Nucl. Phys. B **629**, pp. 323-392 (2002)
- [6] S. V. Goloskokov and P. Kroll, Eur. Phys. J. A **47**, pp. 112-127 (2011)
- [7] B. Andersson et al., Phys. Rep. **97**, pp. 31-145 (1983)